

# B O L T   B E R A N E K   A N D   N E W M A N   I N C

C O N S U L T I N G   •   D E V E L O P M E N T   •   R E S E A R C H

Job No. 12126

STUDIES OF MANUAL CONTROL SYSTEMS

Progress Report No. 6

for the Period 19 October 1964 to 18 January 1965

RECEIVED  
APR 19 9 31 AM '65  
OFFICE OF GRANTS &  
RESEARCH CONTRACTS

|                   |                               |                    |
|-------------------|-------------------------------|--------------------|
| FACILITY FORM 802 | N65-21766                     | (ACCESSION NUMBER) |
|                   | 37                            | (THRU)             |
|                   | CL-62251                      | (CODE)             |
|                   | (NASA CR OR TMX OR AD NUMBER) | (CATEGORY)         |

19 March 1965

GPO PRICE \$ \_\_\_\_\_  
OTS PRICE(S) \$ \_\_\_\_\_  
Hard copy (HC) \$ 2.00  
Microfiche (MF) .50

Submitted to:

National Aeronautics and Space Administration  
600 Independence Avenue  
Washington, D. C. 20546

Attention: Dr. T. L. K. Small

STUDIES OF MANUAL CONTROL SYSTEMS

PROGRESS REPORT NO. 6

for the Period 19 October 1964 - 18 January 1965

Contract NASw-668

19 March 1965

Submitted to:

National Aeronautics and Space Administration  
600 Independence Avenue  
Washington, D. C. 20546

Attention: Dr. T. L. K. Small

## STUDIES OF MANUAL CONTROL SYSTEMS

### I. INTRODUCTION

This is a report of the work we have done under Contract NASw-668 during the three-month period beginning 19 October 1964 and ending 18 January 1965, the third quarter of the second year of the contract.

The report presents the results of an experiment designed to investigate interaction occurring in a two-axis, mixed-dynamics tracking task. Our test hypothesis was that tracking performance in a given axis would not differ in the following two situations: (1) when that axis alone was tracked, and (2) when an additional axis having dissimilar dynamics was simultaneously tracked. There were three test conditions: (1) X-axis tracking alone with acceleration dynamics; (2) Y-axis tracking alone with position dynamics; (3) two-axis tracking with acceleration in the X-axis and position in the Y-axis. Performance has been quantified in terms of normalized mean-squared error and in terms of describing functions.

In the previous progress report (Report No. 5, dated 1 December 1964) we mentioned a preliminary experiment which showed a degradation of performance in both axes in going from the single-axis to the two-axis condition. Our observations were inconclusive at that time, because the subject

had not been fully trained in the mixed-dynamics task. The experiment was repeated under well-controlled conditions during this past report period, and data were taken only after the subject had reached asymptotic performance. The results of this experiment indicate that the hypothesis as stated in the previous paragraph should be rejected. The normalized error in the position axis was more than doubled by the addition of the second axis; this effect was significant to below the 0.005 level. This increase in error was accompanied by a corresponding change in the human operator's describing function. There was also a degradation of about 10 percent in the acceleration axis in going from the single-axis to the two-axis task. |

## II. EXPERIMENTAL DESIGN

This section presents details of equipment and procedure that are applicable to the particular experiment under review. The reader is referred to Section II of Progress Report No. 5 for a fuller description of the tracking apparatus.

Tracking was compensatory, with acceleration dynamics in the horizontal axis (X-axis) and position control in the vertical axis (Y-axis). The control-display relationships were 64 cm of error displacement per second<sup>2</sup> per centimeter of stick displacement in the X-axis, and 3.2 cm/cm in the Y-axis.\* These numerical values were chosen so that the control effectiveness (CE) would lie between 5 and 10 in each axis. The CE was defined for the X-axis to be the maximum dot acceleration obtainable from the control divided by the RMS acceleration of the forcing function; the Y-axis CE was defined as the maximum dot deflection divided by the RMS of the forcing function.

Since the control stick had no mechanical stops to limit its deflection, the maximum obtainable acceleration or position

---

\*These numbers represent the transfer function of the stick (4-volts output per cm of stick deflection) cascaded with the controlled element dynamics ( $16/s^2$  for the X-axis and 0.8 for the Y-axis). The human operator describing functions presented in the next section include the stick transfer function.

was arbitrarily determined by choosing 3 pds (equivalent to 3 cm of stick deflection) as the maximum force to be applied by the operator. This force was never exceeded during the experimental trials. The CE was maintained roughly the same in the two axes in order to minimize cross-coupling in the operator's motor system.

The input signals were pseudo-Gaussian with augmented rectangular spectra. The bandwidths of the primary and secondary component were 4 and 9 rad/sec, and RMS signal levels in terms of dot motion were 2.0 and 0.1 cm, respectively. The statistics of the X and Y forcing functions were identical, although the waveforms were uncorrelated.

A single subject was employed in this experiment. He was trained until he appeared to reach an asymptotic level of performance in each condition. Data-taking required a total of 27 trials (108 minutes of tracking) presented in a balanced order. The trials were grouped into nine sessions each of which consisted of three 4-minute trials separated by 1-minute rest periods. The experimental plan is indicated in Table I.

The conditions were identical within a given session, but were varied from session to session. In order to facilitate a direct comparison between single- and two-axis performance, the input (forcing function) on a given axis was identical for all trials in which that axis was tracked. The X and Y inputs were different from each other, however.

The circle diameter was varied to provide the subject with a continuous indication of his performance on a mean-squared

error criterion. This procedure has been described in the preceding progress report. The "circle gain" (i. e., the relationship between squared error and diameter) was not constant, but was adjusted inversely to the difficulty of the task so that the subject would see the same average circle diameter and hence would have the same incentive when tracking with acceleration control. When the subject tracked the two axes simultaneously, the X and Y circle gains were weighted on the basis of the single-axis results so that

- (1) the average circle diameter in the two-axes task would be the same as in each of the single-axis tasks, and
- (2) the errors on the two axes would contribute equally to the diameter.

Thus, if a circle gain of  $K_x$  were needed to maintain an average circle diameter of 0.6 cm in the single-axis acceleration task, and a gain of  $K_y$  were needed to maintain a similarly sized circle in the single-axis position task, the circle gains in the two-axes task would be  $K_x/2$  in the X-axis and  $K_y/2$  in the Y-axis. This procedure was adopted to encourage the subject to attend equally to the two tasks even though they were unequal in difficulty, since we found during training that the degradation in performance in the axis with positional control was noticeably greater when the axes were weighted evenly than when they were weighted as just described. Presumably the subject was devoting the larger portion of his efforts to the more difficult of the two tasks.

### III. RESULTS

#### A. ERROR SCORES

The normalized mean-squared error was computed by dividing the mean-squared error of a trial by the corresponding mean-squared input. The scores obtained during the 27 experimental runs are plotted in Fig. 1. With the exception of the first session (Trials 1-3) the performance was remarkably stable and showed no learning trend. The relatively higher scores of the first session indicate either that the subject was not fully warmed up at the start of the data-taking, or that he modified his tracking strategy to suit the particular test signals during that session.

The mean errors and their standard deviations have been estimated from the error scores and are presented in Table II. The ratio  $\Delta M / \sigma_M$  was used to estimate the statistical significance of the differences between one- and two-axis errors.  $\Delta M$  is the difference between mean errors and  $\sigma_M$  is the estimated standard deviation of this difference. The X-axis ( $K/s^2$ ) results are significant at the .025 level, whereas the Y-axis (K) results are significant to below the 0.005 level on the assumption that the scores have a t distribution. Two measures of the percentage difference between single-axis and two-axis tracking are provided. If we take the average of the single-axis and two-axis performances as the basis for comparison, the difference between single-axis and two-axis



performance is 12.6 percent in the X-axis and 77 percent in the Y-axis. When the single-axis performance is the basis for comparison, the percentage increase in error in the two-axis task is 13.5 percent in the X-axis and 125 percent in the Y-axis. Thus, two-axis tracking with asymmetrical dynamics produces a relatively large and statistically significant degradation in performance in the axis with positional control. There is also a significant, but much smaller, degradation in performance in the axis with acceleration control. Possible explanations for these results are presented in Section IV.

#### B. BODE PLOTS

##### Y-Axis Performance

Figure 2 contains samples of Bode Plots obtained on the Y-axis during single-axis and two-axis tracking. These plots represent the linear relationships between Y-axis error and Y-axis output. Since the controlled element was a pure gain, the error-to-output describing function is identical to that of the human operator (error-to-stick) except for a gain constant.

The six curves represent human controller characteristics obtained with the same segment of the forcing function. The measurements began two minutes following the onset of the signal and lasted for 30 secs. Each curve represents a different experimental run. Curves a, c, and e were obtained during Trials 13-15; curves b, d, and f were obtained during Trials 16-18.

Bode Plots of Fig. 2 are compared in Fig. 3 in which is indicated the range of gain and phase spanned by the three single-axis plots and the three two-axis plots. The results of the single-axis task show a narrower spread than the two-axis results. In the range of frequency in which the input energy is significant (i. e., between  $1/4$  and  $4$  rad/sec), the spread in gain among the single-axis plots is less than 3 db, whereas for the two-axis results it ranges up to 6 db. The phase curves are remarkably consistent, varying by less than 20 degrees (in the single-axis task) and less than 45 degrees in the two-axis task at frequencies below 4 rad/sec.

There is a consistent difference in the amplitude ratios between the two tracking situations. The single-axis AR is about 6 db higher on the average than the two-axis AR at frequencies below 4 rad/sec. The curves are essentially coincident at higher frequencies. The two-axis phase plots indicate lead at frequencies below  $1/2$  rad/sec and show less phase lag than the single-axis curves over the entire frequency range. The gain-crossover frequency is around 10 rad/sec for both single-axis and two-axis tracking. The phase-crossover frequency is around 6 rad/sec in the single-axis task and 8 rad/sec in the two-axis task. Since phase crossover occurs at lower frequencies than gain crossover, the subject has exhibited a negative phase margin: roughly 60 degrees in the single-axis situation and 40 degrees in the two-axis case.

One explanation for the negative phase margin is that it is an anomaly of the measurement technique. Since there is an

insignificant amount of error power at 10 rad/sec (about 18 db less than the power at low frequencies) the analysis filters can make a poor approximation to the describing function in that region of frequency without significantly degrading the match (on a mean-squared error basis) between filter output and human operator output.

The differences in Bode Plots correspond well with differences in error scores. A set of normalized mean-squared errors was computed which correspond to the same input segment from which the Bode Plots were obtained. The average of the three single-axis scores was 0.029; the two-axis scores averaged to 0.082. In order to compute the errors expected on the basis of the Bode Plots, the describing functions were approximated by pure gains. This approximation is reasonable since the amplitude ratios are fairly flat over the range of significant signal energy.

The averages of the amplitude ratio curves over the range of 1/4 to 4 rad/sec were 13.5 db for the single-axis plots and 9.0 db for the two-axis results, corresponding to ratios of 5.63 and 2.82. If the system is essentially linear, the normalized mean-squared error should equal the square of the transfer function from input to error. Thus

$$\frac{\overline{e^2}}{\overline{i^2}} = \left| \frac{1}{[1+HC]} \right|^2$$

which yields normalized errors of 0.030 and 0.068 for the single- and two-axis situations, respectively.

Figure 4 shows Bode Plots obtained from successive segments of the same run. Since the differences among describing functions obtained from successive segments in the same trial are greater than the differences seen in plots obtained from identical segments of successive trials, such differences are likely to reflect changes in operator behavior, or measurement artefacts caused by the nature of the particular segment of forcing function. We showed this to be the case in the previous progress report. The differences between single-axis and two-axis plots, however, are similar for all three segments. The single-axis and two-axis results corresponding to the fourth and fifth segments are plotted on a common set of axes for comparison in Figs. 5 and 6.

#### X-Axis Performance

Six human operator describing functions, representing the responses to identical segments of forcing functions, are displayed in Fig. 7; plots a, c, and e are for single-axis tracking (Trials 10-12) and b, d, and f are for two-axis tracking (Trials 16-18). The input segments for all of these describing functions were the same and coincided with the segment used to obtain the curves of Fig. 2.

The two-axis gain and phase plots differ in appearance from the single-axis curves in that the latter show pronounced fluctuations in the neighborhood of  $1/2$  rad/sec. The composite plot of Fig. 8 shows, however, that this difference in appearance does not represent a major difference in system performance. The single-axis and two-axis curves are similar

in form over the range of significant signal energy (1-8 rad/sec); the single-axis amplitude ratio is from 1 to 3 db higher than the two-axis AR. Note that the energy in the error signal is correlated in a higher frequency region when the controlled element is second-order than when it is pure gain. Specifically, the open-loop gain is so great at frequencies below 1 rad/sec that wide variations in human operator characteristics in this region will have little effect on overall performance.

The open-loop describing functions ( $H_x C_x$ ) corresponding to Figs. 7c and 7d are plotted in Fig. 9. This set of curves was obtained by cascading the human describing functions with  $16/s^2$ , the controlled element, for which pair of describing functions there is no noticeable difference between the single-axis and two-axis results above 1 rad/sec. This is to be expected since the normalized errors corresponding to these curves are the same (0.11). Unlike the Y-axis describing functions, these show a positive phase margin of 10 to 20 degrees. Gain crossover occurs around 6 rad/sec.

Human operator describing functions for three successive segments of the same run are shown in Fig. 10. Variations with respect to signal segment are minor between 1 and 8 rad/sec. Figures 11 and 12 show that variations with respect to number of axes tracked are also small over that frequency range; the gains are within 3 db and the phase lags vary less than 15 degrees.

Closed-loop describing functions (input-output) are shown for both the X- and Y-axes in Fig. 13. Figures 13a and 13b

correspond to the Y-axis open-loop describing functions of Figs. 2c and 2d; Figs. 13c and 13d correspond to the X-axis curves of Figs. 7c and 7d, and Fig. 9. The amplitude ratio of Fig. 13b is uniformly lower than that of Fig. 13a, which reflects the differences between the single- and two-axis open-loop amplitude ratios shown in Fig. 3. The X-axis plots of Figs. 13c and 13d indicate very tight control at low frequencies, as could be predicted from the high, open-loop gains seen in Fig. 9. However, a resonant peak is seen around 8 rad/sec (the open-loop phase-crossover frequency).

## IV. DISCUSSION

We have shown that when the X-axis dynamics were  $K/s^2$  and the Y-axis dynamics were  $K$ , the Y-axis performance suffered a noticeable degradation in going from the single-axis to the two-axis situation, whereas the change in X-axis performance was relatively minor. This asymmetric interaction between the axes occurred despite the following attempts to equalize the interaction. First, the control effectiveness in each axis was weighted so that the RMS stick movements would be similar in the two axes. This procedure was intended to equalize the mechanical interaction, i. e., the occurrence in one axis of motions that were intended solely for the other axis. Secondly, the circle gains were weighted so that the operator would concentrate equally on the two tasks. We feel, therefore, that the observed asymmetric interaction is a significant result.

Our model of the human controller is divided into three major components: (1) the information input, (in this experiment, the eyes), (2) the central controller (the central nervous system), and (3) the effector outputs (in this experiment, the hand and its effector muscles). The degradation of the Y-axis ( $K$ ) performance in the mixed-dynamics task may reflect the limitations of a single component or of a combination of components. The following hypotheses, some of which were discussed in the previous report, are offered as possible explanations for the observed interaction.

1. Limitations in the visual system are important.
2. Information processing capabilities of the central controller are overloaded.
3. The organizational capabilities of the central controller are stressed; the subject cannot generate the required transfer functions when two different transfer functions must be generated simultaneously.
4. Interaction occurs in the effector outputs; the subject cannot control his motor responses precisely enough to prevent motions intended for a given axis from introducing components of motion in the other axis.
5. The subject concentrates primarily on reducing the X-axis errors in the two-axis task because these errors are noticeably greater than the Y-axis errors.

These hypotheses are discussed in order in the following paragraphs. On the basis of present knowledge, all but the fifth hypothesis can be rejected as representing significant effects.

1. Limitations of the visual system. There was no limitation due to sampling between the axes, since the two-dimensional display allowed the subject to observe both components of the error simultaneously. The subject may have had perceptual difficulties in the two-axis task; this possibility will be discussed with hypothesis 5.



2. Information overloading. The degradation in the Y-axis performance does not reflect purely an overloading of the information processing capabilities of the central controller. We have shown in previous experiments that the same subject was able to track each of two axes in a two-axis task as well as either axis alone when the dynamics on the two axes were identical. Specifically, the errors on either axis of a two-axis task with K dynamics on both axes were less than the errors on either axis of the mixed-dynamics task. Since the rate of information transmitted is inversely related to the tracking error, the rate at which the subject was inherently capable of transmitting information was greater than the rate at which information was transmitted in the mixed-dynamics situation.

3. Organization of two describing functions. The subject had a complex organizational task. In order to maintain roughly the same open-loop (error-to-output) describing function, which he had to do in the region of gain crossover, he had to simultaneously generate describing functions on X and Y that differed by two integrations. If the central processor were not able to meet this requirement fully, the X-axis describing function in the two-axis task might be expected to assume some of the characteristics associated with the Y-axis describing function in the single-axis task, and vice versa; that is, the X and Y human operator describing functions obtained from two-axis tracking would resemble each other more closely than those obtained from single-axis tracking.

This effect was present to some extent. Figures 2b, 4d, and 4f show a low-frequency lead in the position-axis describing functions for the two-axis situation. Such a lead is characteristic of tracking with acceleration dynamics, but not with position dynamics in the one-axis task. On the other hand, the most significant difference between the single-axis and two-axis describing functions is a relatively uniform difference in amplitude ratio. This behavior suggests that the operator is doing the same type of thing on the Y-axis in the two-axis task as in the single-axis task, but less effectively. On the whole, the requirement of simultaneously organizing two different describing functions does not appear to be a major limiting factor.

4. Motor interaction. Even though the control effectiveness on each axis was adjusted so that the stick motions in the two axes would have roughly the same RMS amplitudes, the nature of the control motions was quite different. The X-axis stick motion contained primarily high-frequencies, whereas the Y-axis response contained mainly low-frequencies, which behavior followed from the requirement of generating a lead on the X-axis and a lag on the Y-axis. Thus, one might expect that in the two-axis situation the rapid stick motions intended for the X-axis might spill over into the Y-axis and introduce some high-frequency error there.

Figure 14 shows qualitatively that there is some high-frequency interaction between X and Y stick motions. The three tracings are (a) a segment of Y-axis response (stick motion) obtained from single-axis tracking, (b) the corres-

ponding segment of Y-axis response obtained from two-axis tracking, and (c) the segment of X-axis response coincident with Tracing b. Visual inspection of the Y-axis tracings reveals a component around 3 cps in the two-axis response that is absent in the single-axis response.

A quantitative measure of the high-frequency interaction could be provided by a comparison of the error or stick spectra. On the basis of Figs. 14a and 14b, one would expect to see a relative peak in the two-axis spectrum in the region of 3 cps. Since that frequency was beyond the range of our analysis techniques, we could not examine for such a peak. We did obtain the error power spectra for the Y-axis over the region of significant input energy, however. The single-axis and two-axis spectra are plotted together in Fig. 15; the spectra have been normalized with respect to the low-frequency end of the single-axis curve. The spectra differ almost uniformly over the range of significant frequencies as did the Bode plots. Since the difference between the spectra is large enough to account for the difference between the corresponding mean-squared errors, we conclude that the introduction of high-frequency errors due to the interaction of the X and Y stick motions accounts for a minor part of the difference between the single-axis and two-axis performance on the Y-axis.

5. Uneven Attention: We have shown that the subject exhibited the same type of Y-axis behavior in the two-axis case as in the single-axis case, but to a lesser degree. The simplest conclusion to draw from this finding, and perhaps

the most difficult to quantify, is that the subject concentrates more heavily on the X-axis than on the Y-axis in the two-axis situation because the X-axis errors are bigger. It is quite possible that the subject relaxed his criterion of Y-axis performance despite our attempts to prevent this with unequal settings of circle gains. It is also possible that the subject's perception of Y-axis errors was modified by the presence of larger X-axis errors; that is, the Y-axis errors may have appeared to be smaller in the two-axis situation than when the Y-axis alone was tracked.

## V. EXPERIMENTAL PLANS

We are presently repeating the experiments described in this and previous reports with a number of subjects so that our conclusions will have more general applicability. We hope to investigate more directly the causes of the interaction between axes. One possible experiment is to weight the display gains on the two axes inversely proportional to the average errors. In this situation the subject would see errors of similar magnitudes on the two axes, even though his relative performance (mean-squared error divided by mean-squared input) might be markedly different on the two axes. The intent of this exercise is to test directly the hypothesis that the observed interaction is caused by the subject attending primarily to the axis with the larger errors.

TABLE I  
Experimental Plan

| Session | Run Number     | Task   |
|---------|----------------|--------|
| 1       | 1<br>2<br>3    | 2-axis |
| 2       | 4<br>5<br>6    | X-axis |
| 3       | 7<br>8<br>9    | Y-axis |
| 4       | 10<br>11<br>12 | X-axis |
| 5       | 13<br>14<br>15 | Y-axis |
| 6       | 16<br>17<br>18 | 2-axis |
| 7       | 19<br>20<br>21 | Y-axis |
| 8       | 22<br>23<br>24 | 2-axis |
| 9       | 25<br>26<br>27 | X-axis |

TABLE II

Normalized Mean-Squared Errors  
Acceleration Dynamics on the X-Axis  
Position Dynamics on the Y-Axis

| Axis                           | X-Axis (K/s <sup>2</sup> ) |                       | Y-Axis (K)            |                       |
|--------------------------------|----------------------------|-----------------------|-----------------------|-----------------------|
| Task                           | 1-Axis                     | 2-Axis                | 1-Axis                | 2-Axis                |
| M (Sample Mean)                | .126                       | .143                  | .0371                 | .0832                 |
| $\sigma_M$                     | $2.06 \times 10^{-3}$      | $6.45 \times 10^{-3}$ | $1.64 \times 10^{-3}$ | $2.31 \times 10^{-2}$ |
| $\Delta M = M_2 - M_1$         | .0170                      |                       | .0461                 |                       |
| $\sigma_{\Delta M}$            | $6.77 \times 10^{-3}$      |                       | $2.83 \times 10^{-3}$ |                       |
| $\Delta M / \sigma_{\Delta M}$ | 2.51                       |                       | 16.3                  |                       |
| $\frac{2 \Delta M}{M_1 + M_2}$ | 12.6 %                     |                       | 77 %                  |                       |
| $\frac{\Delta M}{M_1}$         | 13.5 %                     |                       | 124 %                 |                       |

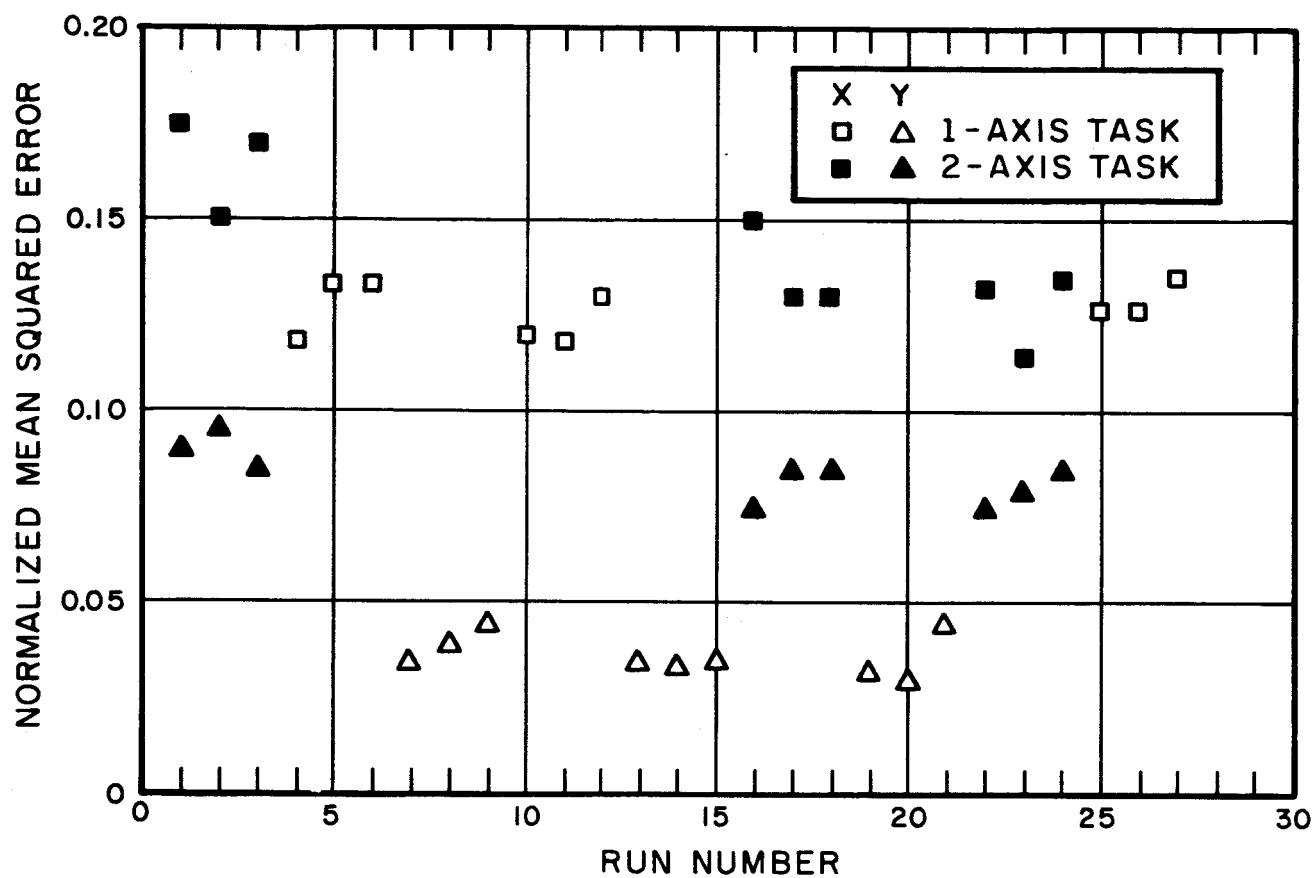


FIG.1 SINGLE-AXIS AND TWO-AXIS PERFORMANCE  
 $C_x = 16/s^2$   $C_y = 0.8$   $w_i = 4 \text{ rad/sec}$

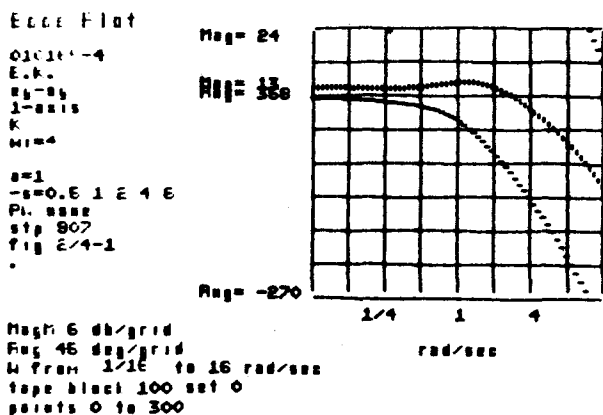


JOB NO. III26

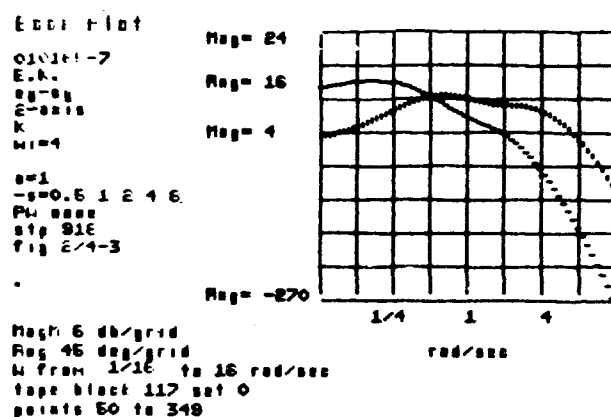
BOLT BERANEK & NEWMAN INC

SINGLE-AXIS TRACKING

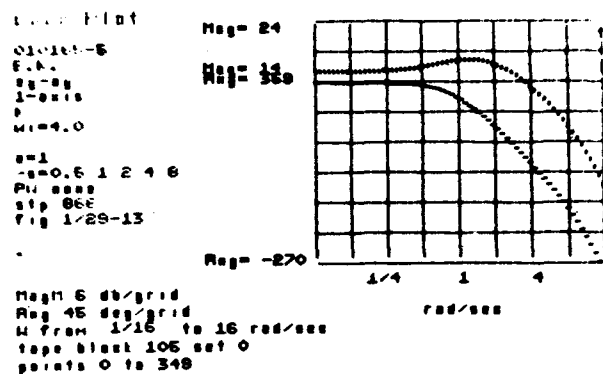
TWO-AXIS TRACKING



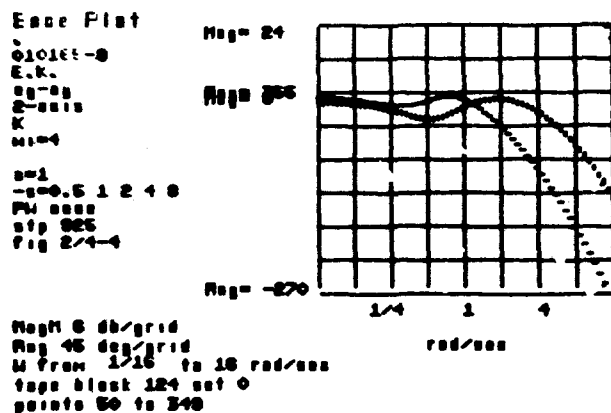
a



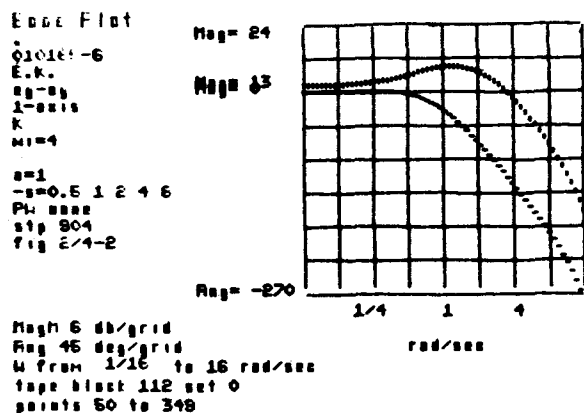
b



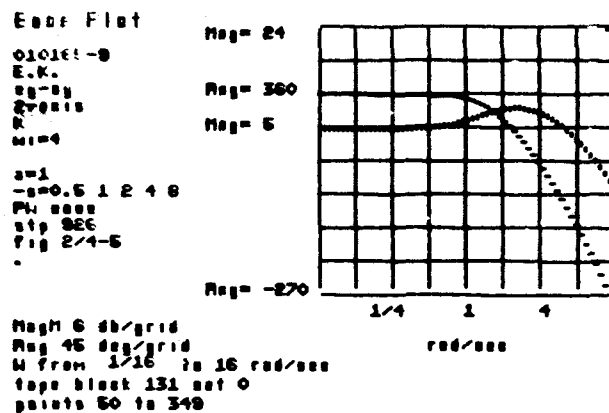
c



d



e



f

FIG.2 OPEN-LOOP DESCRIBING FUNCTIONS, Y-AXIS IDENTICAL SEGMENTS, SUCCESSIVE TRIALS

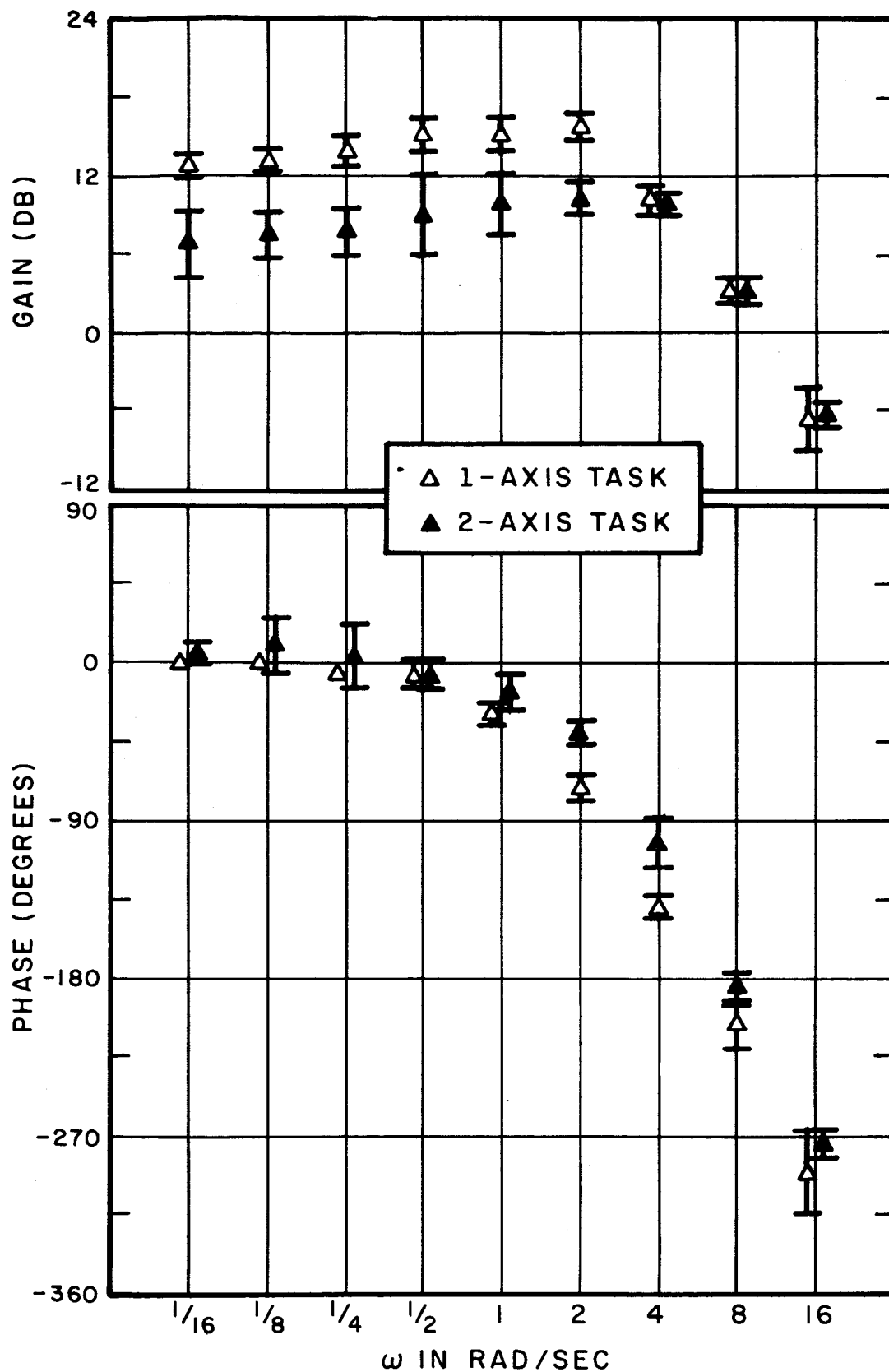
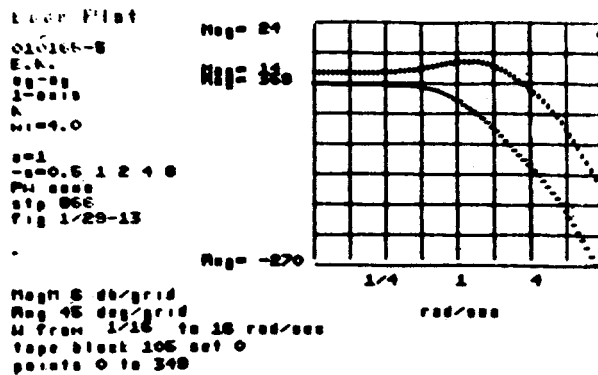


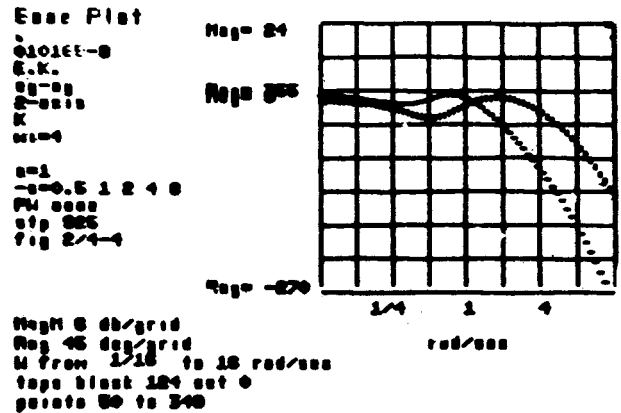
FIG.3 OPEN-LOOP DESCRIBING  
FUNCTIONS, Y-AXIS  
THIRD SEGMENT  
 $C_y = 0.8$

## SINGLE - AXIS TRACKING

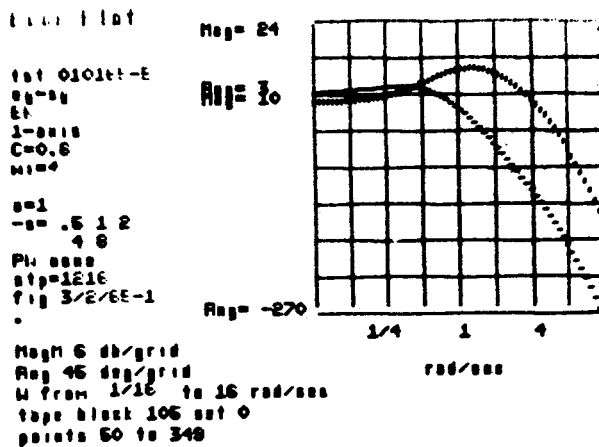


a

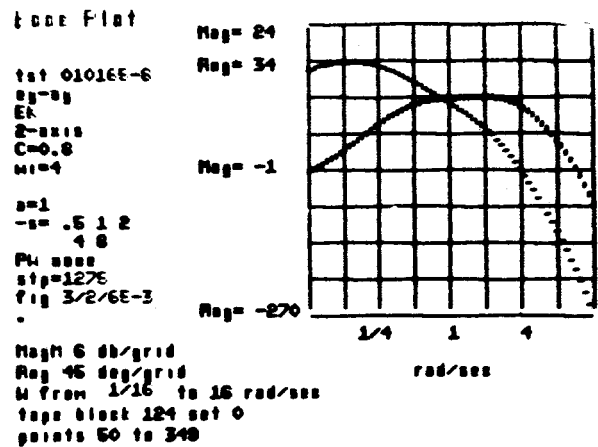
## TWO-AXIS TRACKING



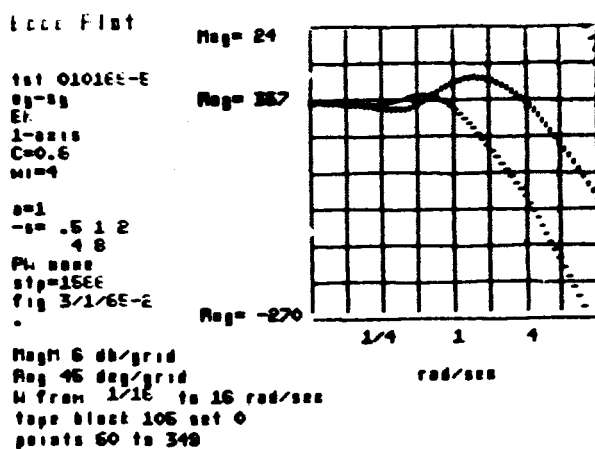
b



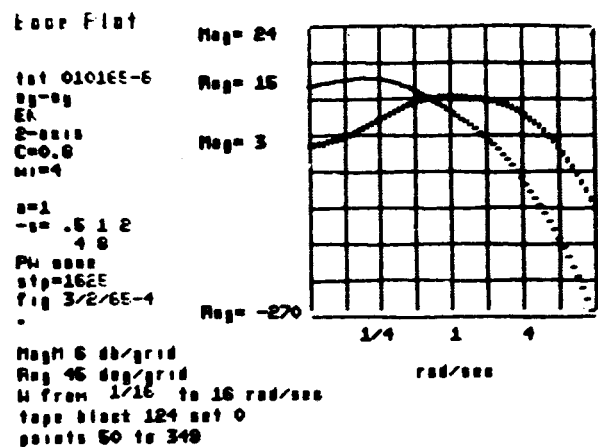
c



d



e



f

FIG.4 OPEN-LOOP DESCRIBING FUNCTIONS, Y-AXIS  
SUCCESSIVE SEGMENTS, IDENTICAL TRIALS

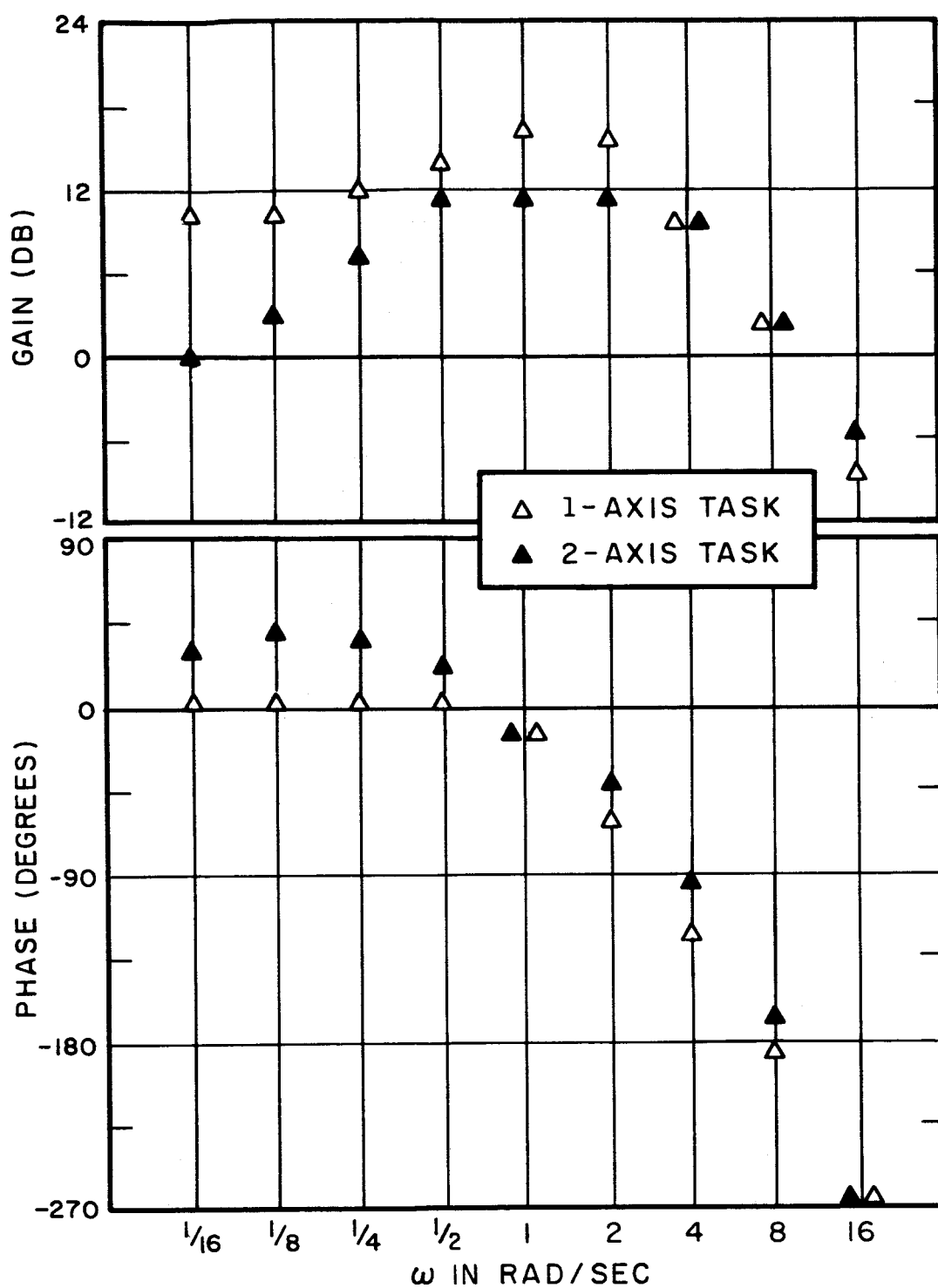


FIG.5 OPEN-LOOP DESCRIBING  
FUNCTIONS, Y-AXIS  
FOURTH SEGMENT  
 $C_y = 0.8$

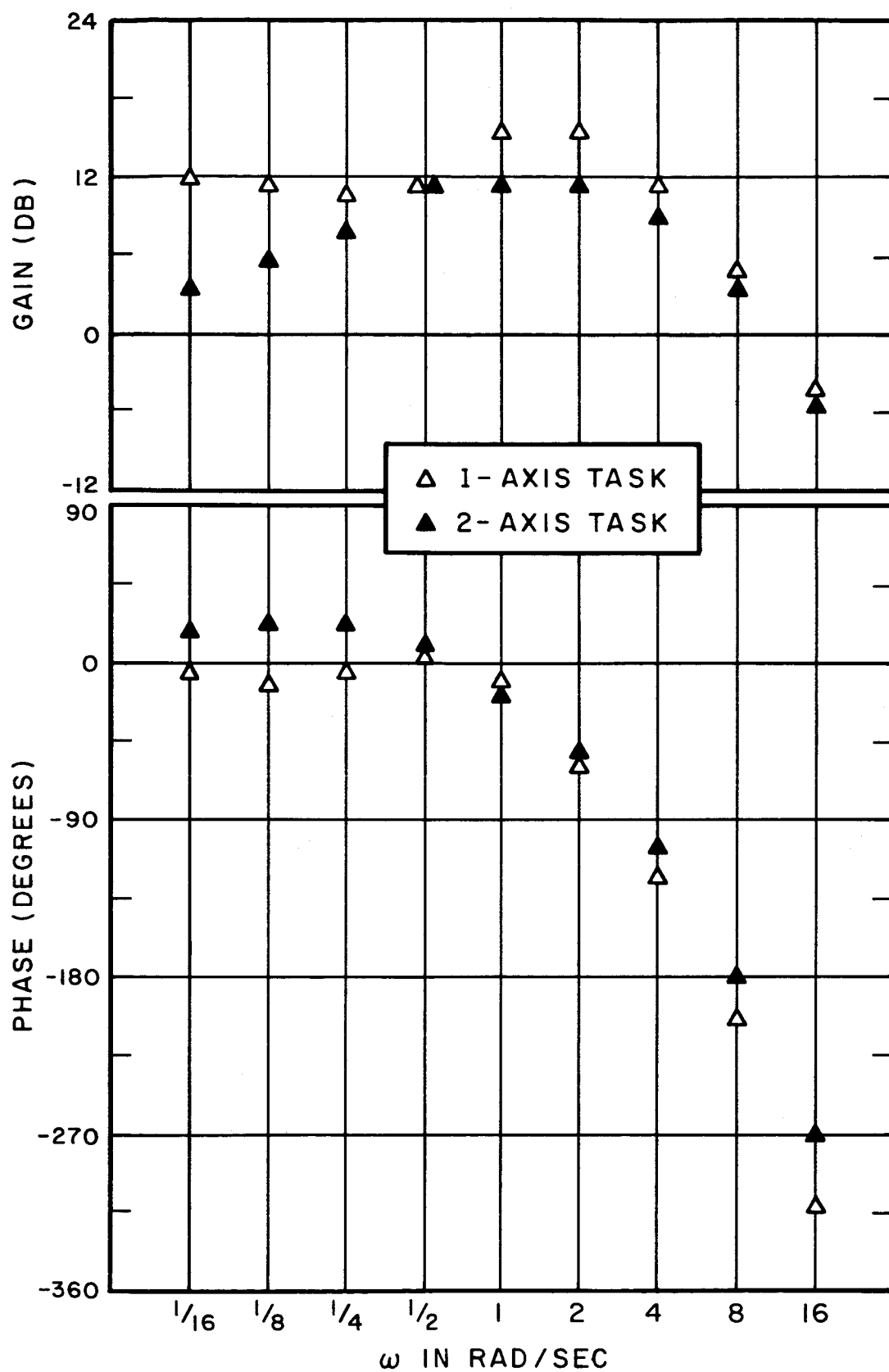
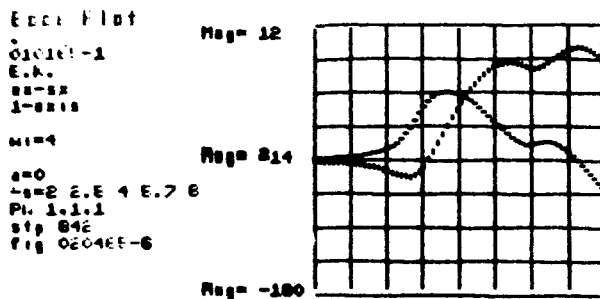


FIG.6 OPEN-LOOP DESCRIBING  
FUNCTIONS, Y-AXIS  
FIFTH SEGMENT  
 $C_y = 0.8$

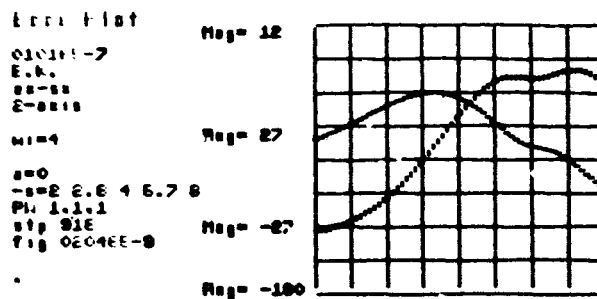
## SINGLE-AXIS TRACKING



Mag 6 db/grid  
Mag 45 deg/grid  
W from 1/16 to 16 rad/sec  
tape block 63 set 0  
points 50 to 349

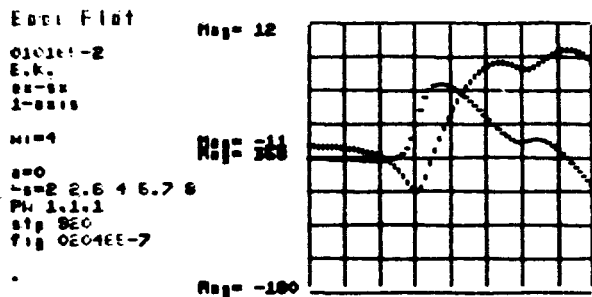
a

## TWO-AXIS TRACKING



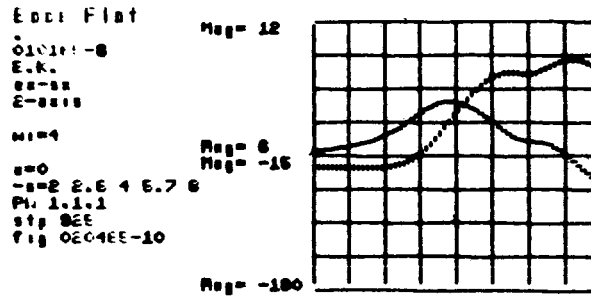
Mag 6 db/grid  
Mag 45 deg/grid  
W from 1/16 to 16 rad/sec  
tape block 117 set 0  
points 50 to 349

b



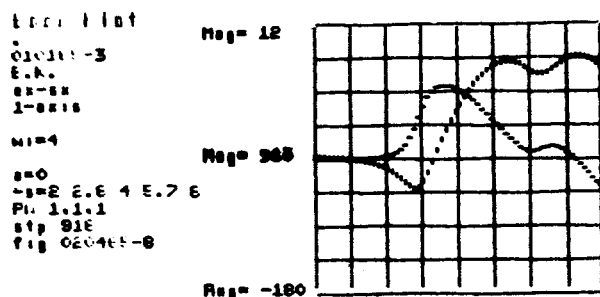
Mag 6 db/grid  
Mag 45 deg/grid  
W from 1/16 to 16 rad/sec  
tape block 66 set 0  
points 50 to 349

c



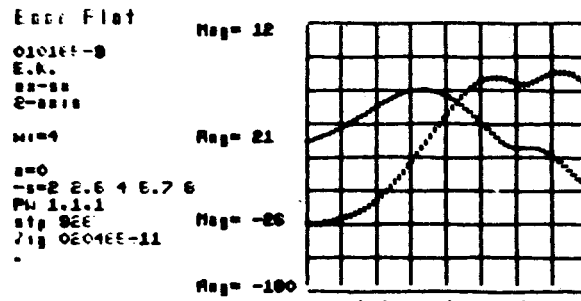
Mag 6 db/grid  
Mag 45 deg/grid  
W from 1/16 to 16 rad/sec  
tape block 124 set 0  
points 50 to 349

d



Mag 6 db/grid  
Mag 45 deg/grid  
W from 1/16 to 16 rad/sec  
tape block 73 set 0  
points 50 to 349

e



Mag 6 db/grid  
Mag 45 deg/grid  
W from 1/16 to 16 rad/sec  
tape block 131 set 0  
points 50 to 349

f

FIG.7 HUMAN OPERATOR DESCRIBING FUNCTIONS, X-AXIS IDENTICAL SEGMENTS, SUCCESSIVE TRIALS

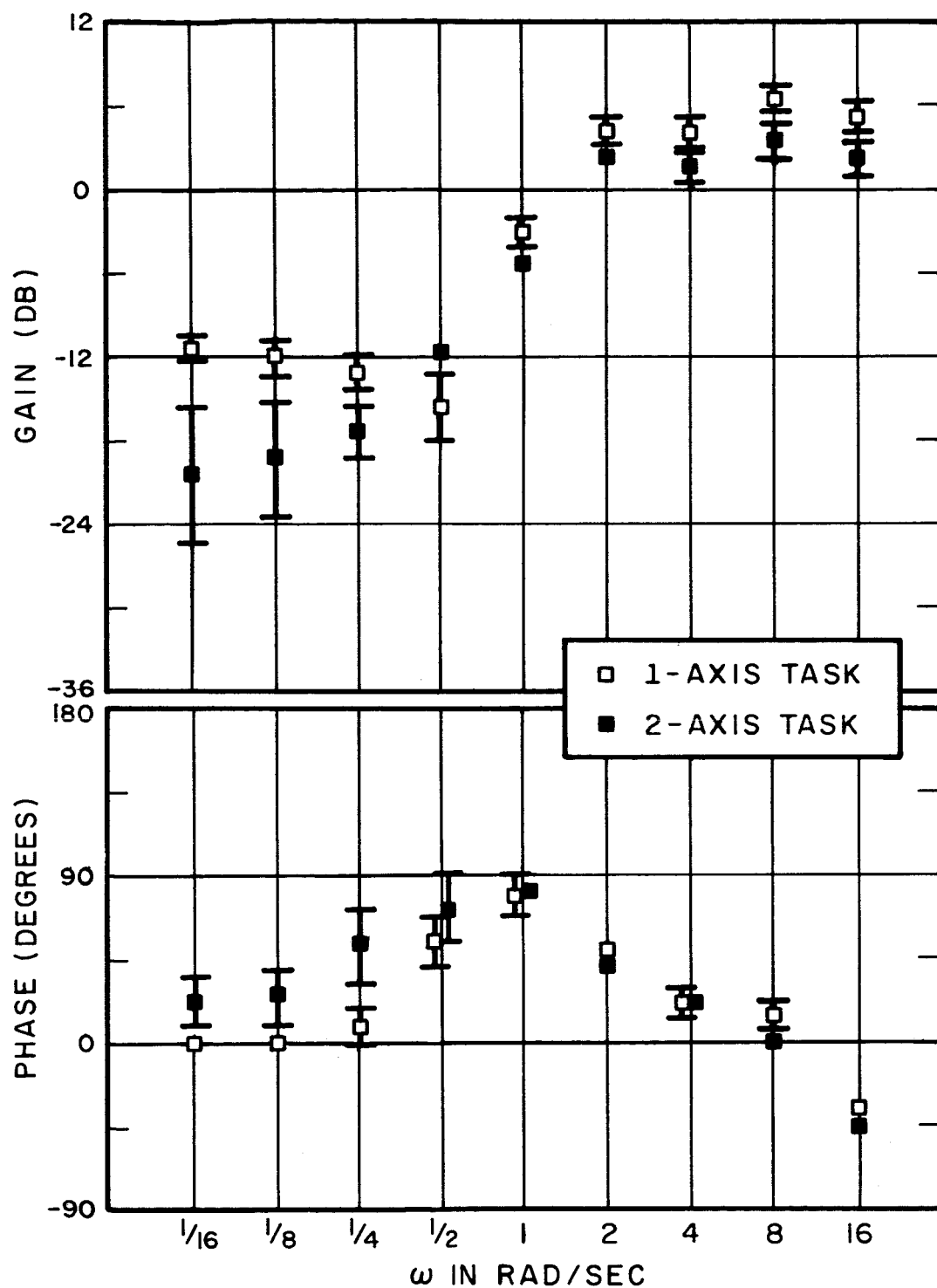


FIG.8 HUMAN OPERATOR DESCRIBING  
FUNCTIONS, X-AXIS  
THIRD SEGMENT  
 $C_x = 16/s^2$

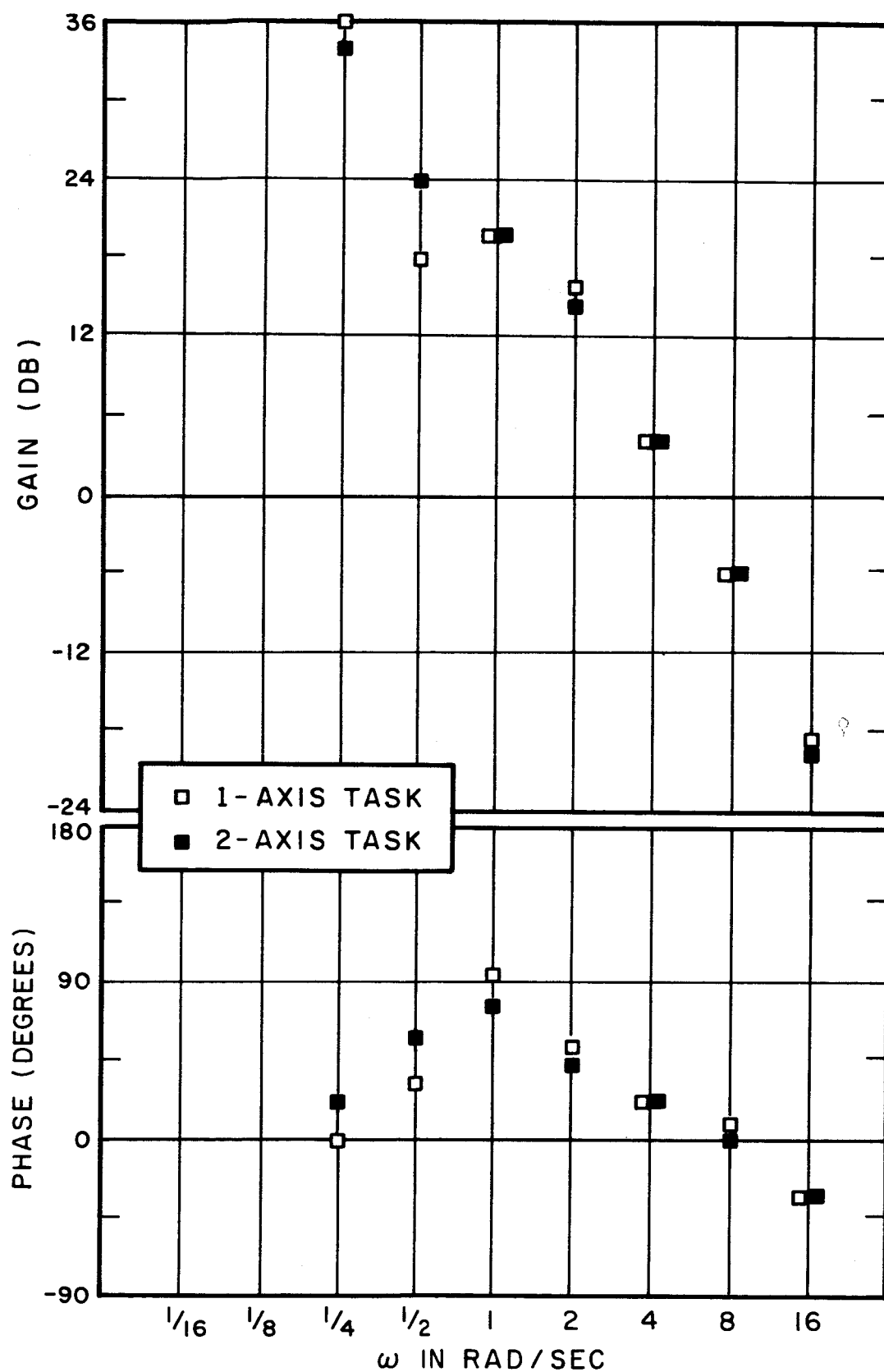


FIG.9 OPEN-LOOP DESCRIBING  
FUNCTIONS, X-AXIS  
THIRD SEGMENT  
 $C_x = 16/s^2$



## SINGLE-AXIS TRACKING

Edge Plot

0101EE-2  
E.K.  
Sx-Sx  
1-axis

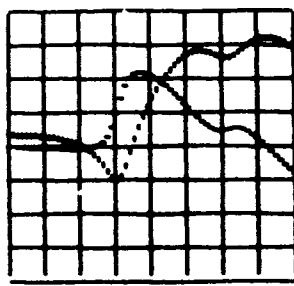
M=4

s=0  
-s=2 2.6 4 5.7 8  
PH 1.1.1  
stp 350  
fig 0204EE-7

Mag= 12

Mag= 36

Mag= -100

Mag 6 db/grid  
Mag 45 deg/grid  
M from 1/16 to 16 rad/sec  
tape block 66 set 0  
points 50 to 348

a

## TWO-AXIS TRACKING

Edge Plot

0101EE-8  
E.K.  
Sx-Sx  
2-axis

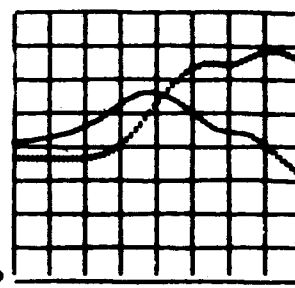
M=4

s=0  
-s=2 2.6 4 5.7 8  
PH 1.1.1  
stp 350  
fig 0204EE-10

Mag= 12

Mag= 36

Mag= -100

Mag 6 db/grid  
Mag 45 deg/grid  
M from 1/16 to 16 rad/sec  
tape block 124 set 0  
points 50 to 348

b

Edge Plot

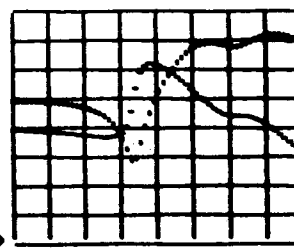
1st 0101EE-2  
E.K.  
Sx-Sx  
K/s2  
M=4s=0  
-s=2 2.6 4 5.7 8  
PH 1.1.1  
stp 1270  
fig 2/2E/6E-2

Mag= 12

Mag= -7

Mag= 36

Mag= -100

Mag 6 db/grid  
Mag 45 deg/grid  
M from 1/16 to 16 rad/sec  
tape block 66 set 0  
points 50 to 348

c

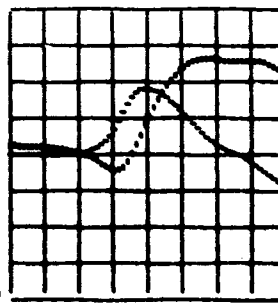
Edge Plot

1st 0101EE-8  
E.K.  
Sx-Sx  
K/s2  
M=4s=0  
-s=2 2.6 4 5.7 8  
PH 1.1.1  
stp 1270  
fig 2/2E/6E-4

Mag= 12

Mag= 36

Mag= -100

Mag 6 db/grid  
Mag 45 deg/grid  
M from 1/16 to 16 rad/sec  
tape block 124 set 0  
points 50 to 348

d

Edge Plot

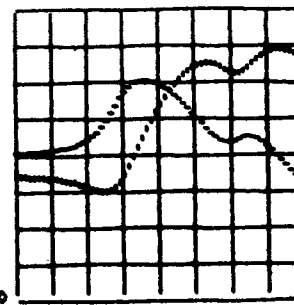
1st 0101EE-2  
E.K.  
Sx-Sx  
K/s2  
M=4s=0  
-s=2 2.6 4 5.7 8  
PH 1.1.1  
stp 1620  
fig 2/2E/6E-3

Mag= 12

Mag= 3

Mag= -17

Mag= -100

Mag 6 db/grid  
Mag 45 deg/grid  
M from 1/16 to 16 rad/sec  
tape block 66 set 0  
points 50 to 348

e

Edge Plot

1st 0101EE-8  
E.K.  
Sx-Sx  
K/s2  
M=4s=0  
-s=2 2.6 4 5.7 8  
PH 1.1.1  
stp 1620  
fig 2/2E/6E-5

Mag= 12

Mag= 3

Mag= -15

Mag= -100

Mag 6 db/grid  
Mag 45 deg/grid  
M from 1/16 to 16 rad/sec  
tape block 124 set 0  
points 50 to 348

f

FIG.10 HUMAN OPERATOR DESCRIBING FUNCTIONS,  
X-AXIS  
IDENTICAL SEGMENTS, SUCCESSIVE TRIALS

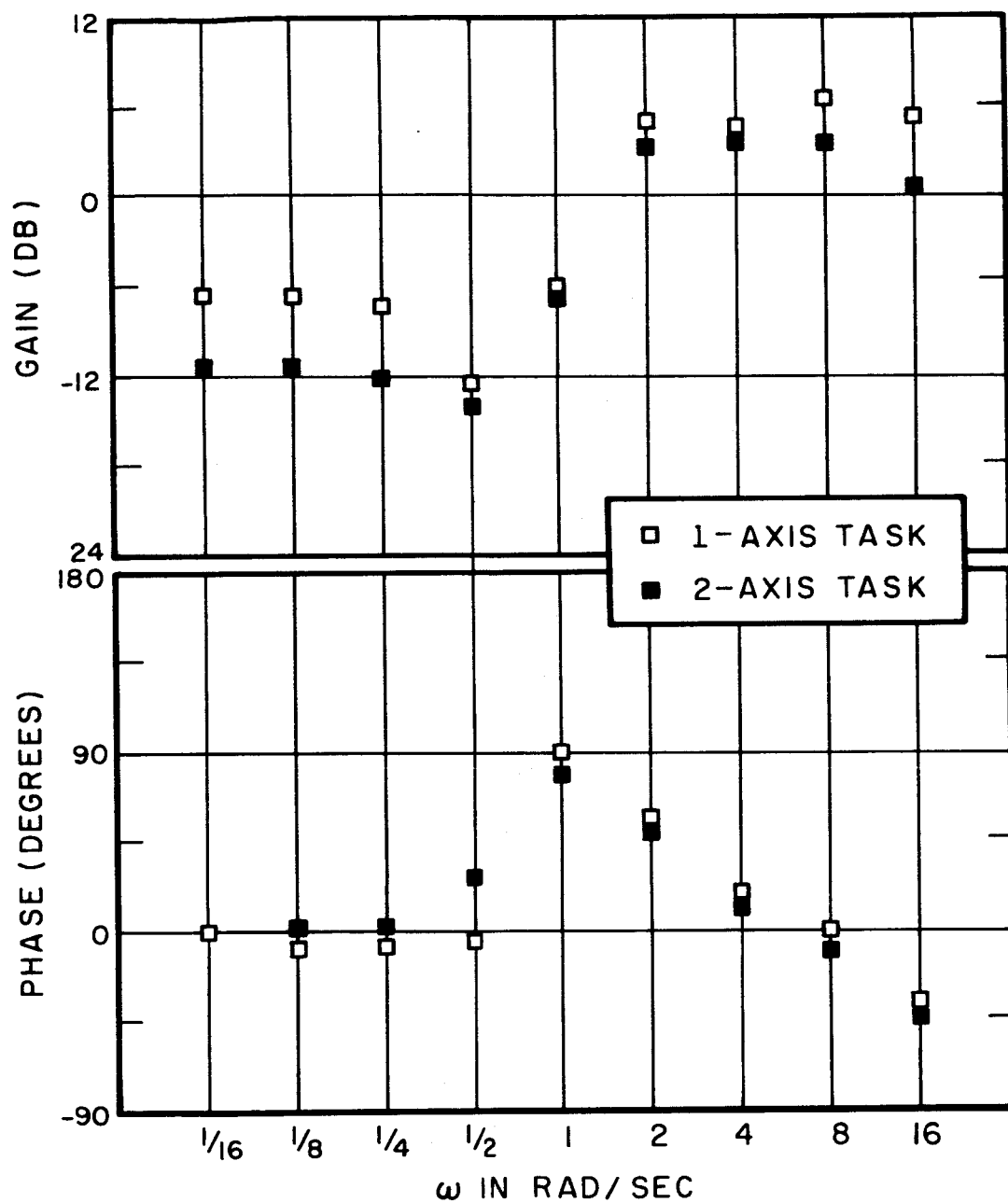


FIG.11 HUMAN OPERATOR DESCRIBING  
FUNCTIONS, X-AXIS  
FOURTH SEGMENT  
 $C_x = 16/s^2$

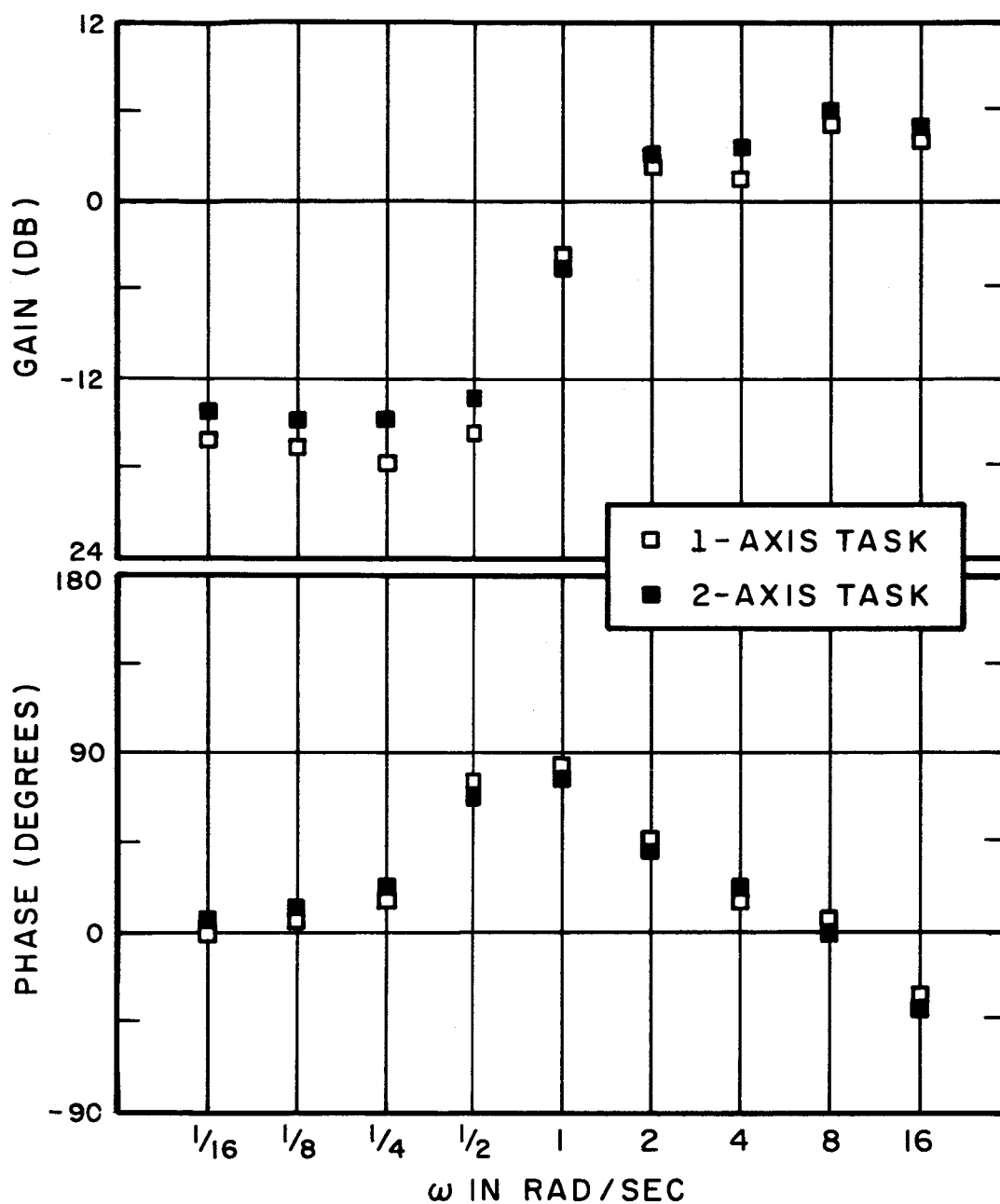
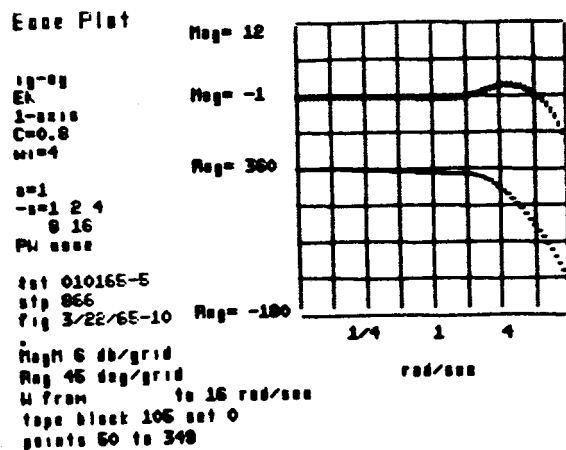


FIG.12 HUMAN OPERATOR DESCRIBING  
FUNCTIONS, X-AXIS  
FIFTH SEGMENT  
 $C_x = 16/s^2$

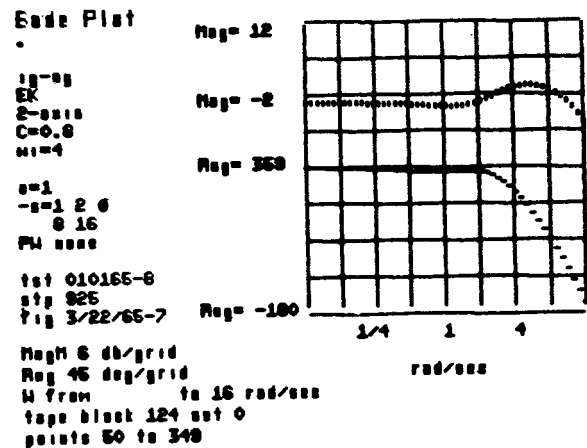
## SINGLE-AXIS TRACKING

## TWO-AXIS TRACKING

## Y AXIS

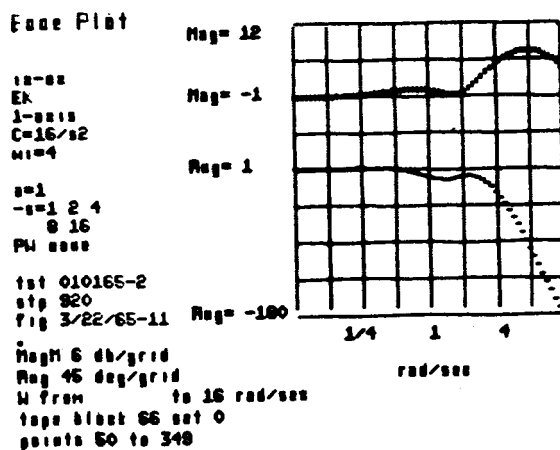


a

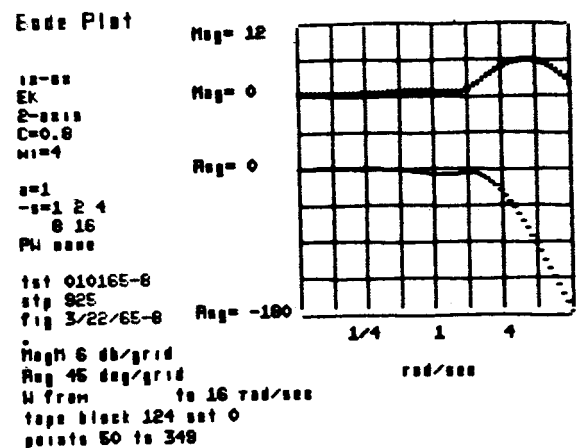


b

## X AXIS



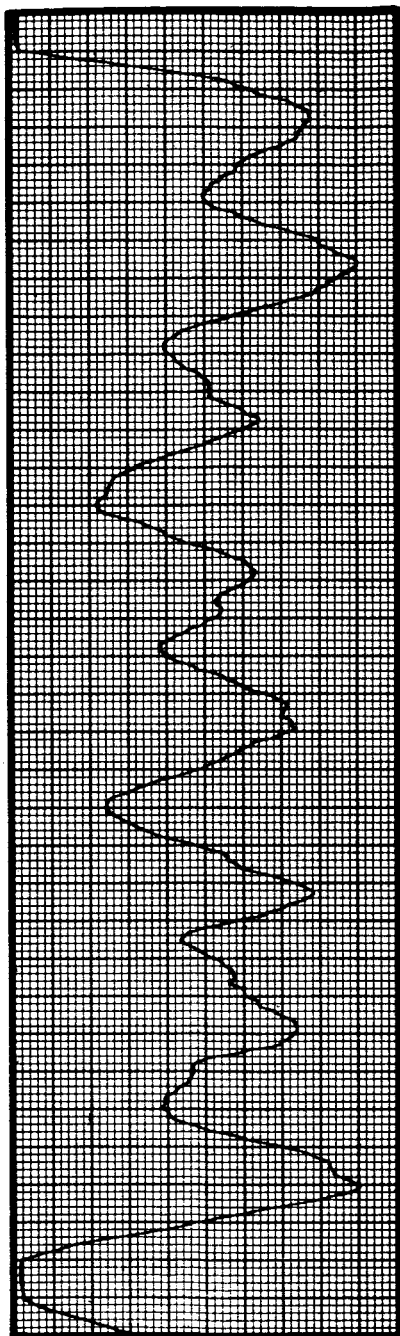
c



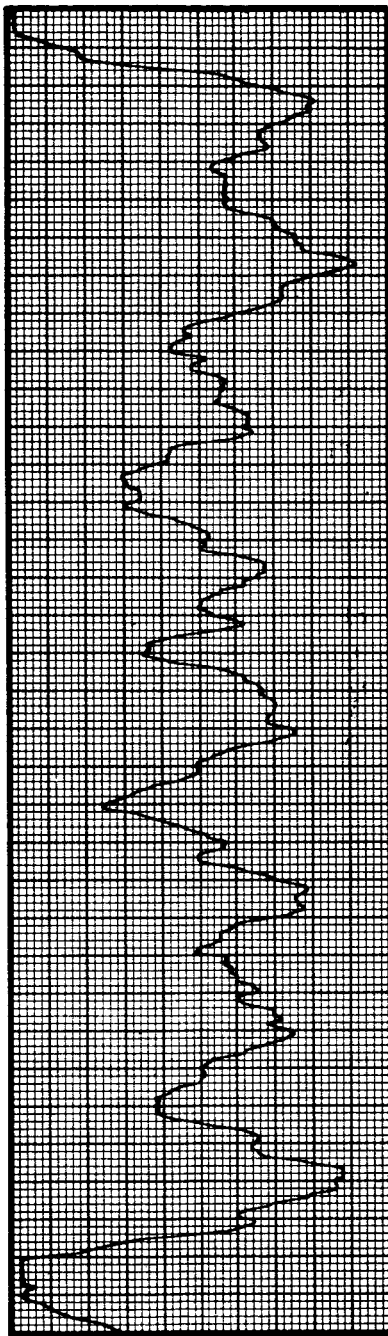
d

FIG.13 CLOSED-LOOP DESCRIBING FUNCTIONS

a: Y-STICK,  
SINGLE-AXIS TASK



b: Y-STICK,  
TWO-AXIS TASK



c: X-STICK,  
TWO-AXIS TASK

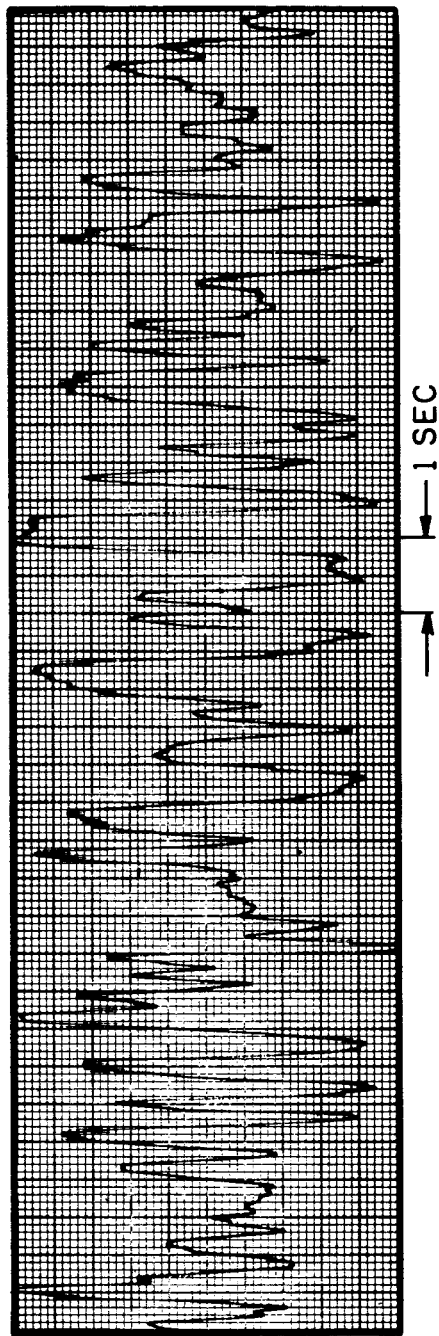


FIG.14 TIME RECORDS OF X AND Y STICK RESPONSES

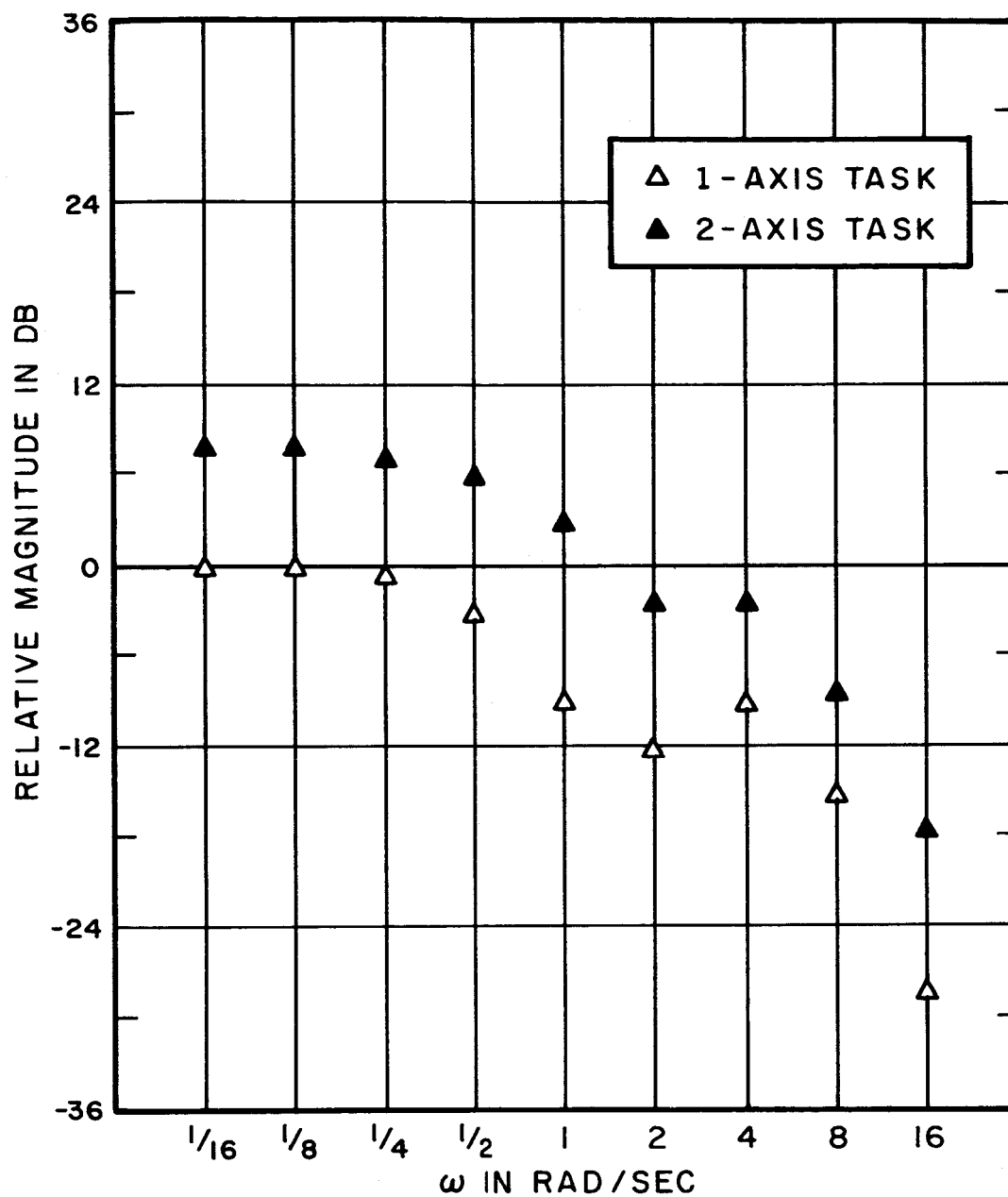


FIG.15 ERROR POWER SPECTRA, Y-AXIS  
THIRD SEGMENT